

Supplementary Material for “Multiscale time-resolved analysis reveals remaining behavioural rhythms in mice without canonical circadian clocks”

Megan Morris, Shin Yamazaki, Aneta Stefanovska

Correspondence to: aneta@lancaster.ac.uk

1 Results

1.1 Oscillatory components

For time-frequency representations of the behavioural data, the signals are first detrended. Then, the wavelet transform is applied using the lognormal wavelet [1] and a frequency resolution parameter of 1.8, for frequencies with periods between 2 minutes and 30.3 hours. A cone of influence is applied. Figs. S1–S3 show the time-frequency representations of behavioural data from mouse 1–5, and the corresponding time-averaged power spectra. The y -axis are in logarithmic scale. Four oscillatory components emerge for all mice. The wavelet power is the squared amplitude of the wavelet, and has, along with the average power, units $(\text{wheel revolutions}/\text{min})^2$.

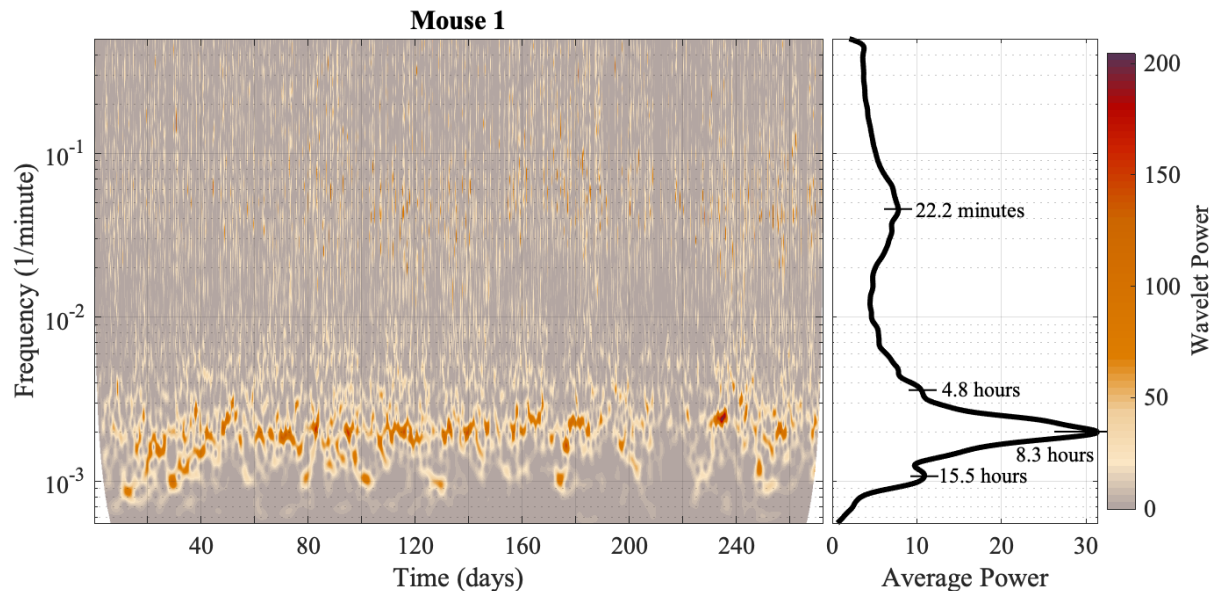


Figure S1: Time-frequency representation (left) and time-averaged wavelet power (right) of the behavioural data for mouse 1.

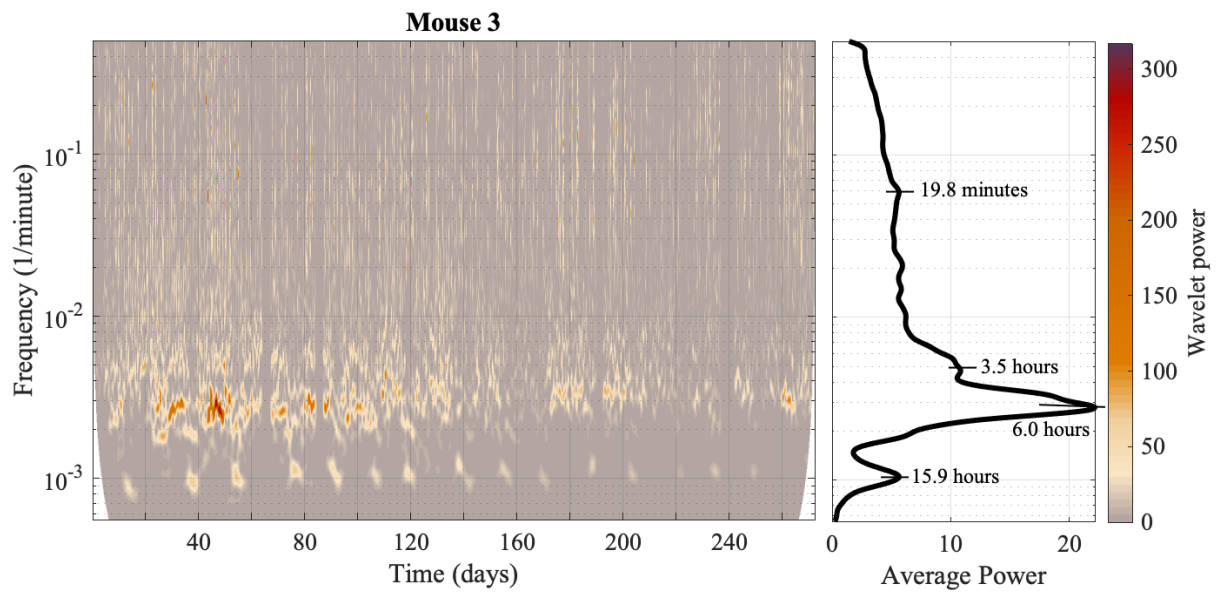
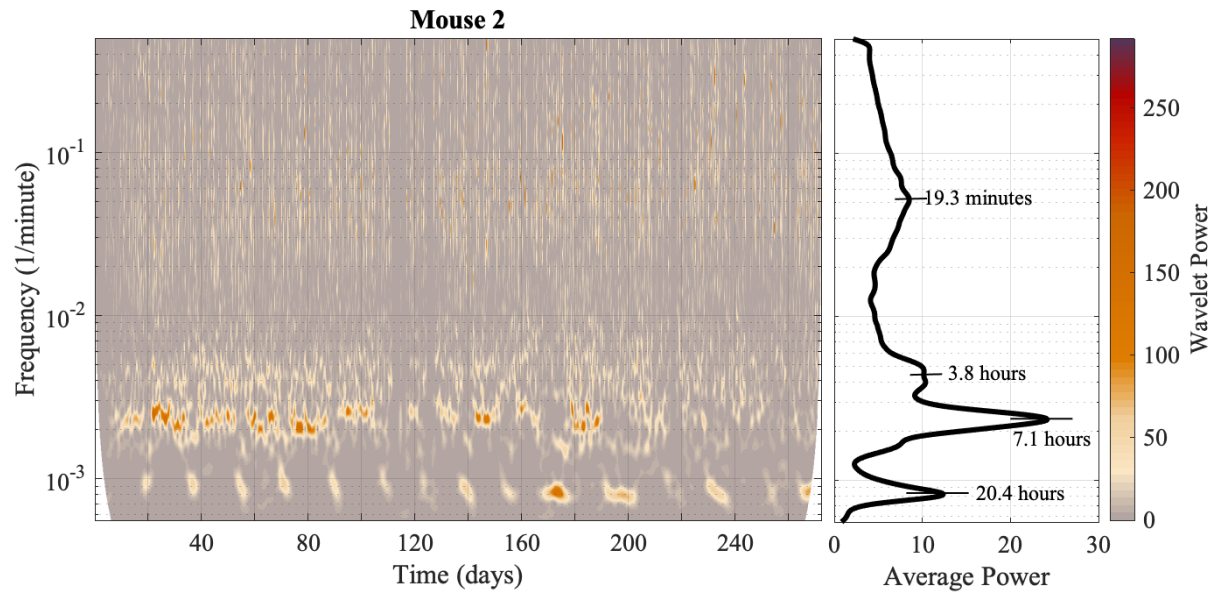


Figure S2: Time-frequency representation of the behavioural data for mice 2 and 3.

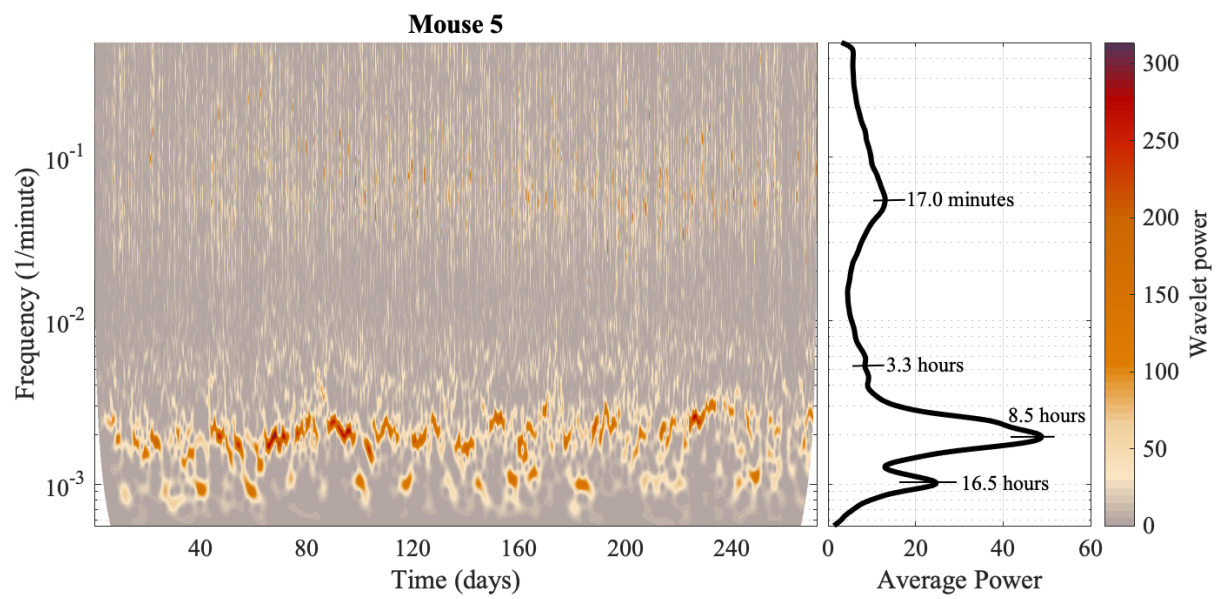
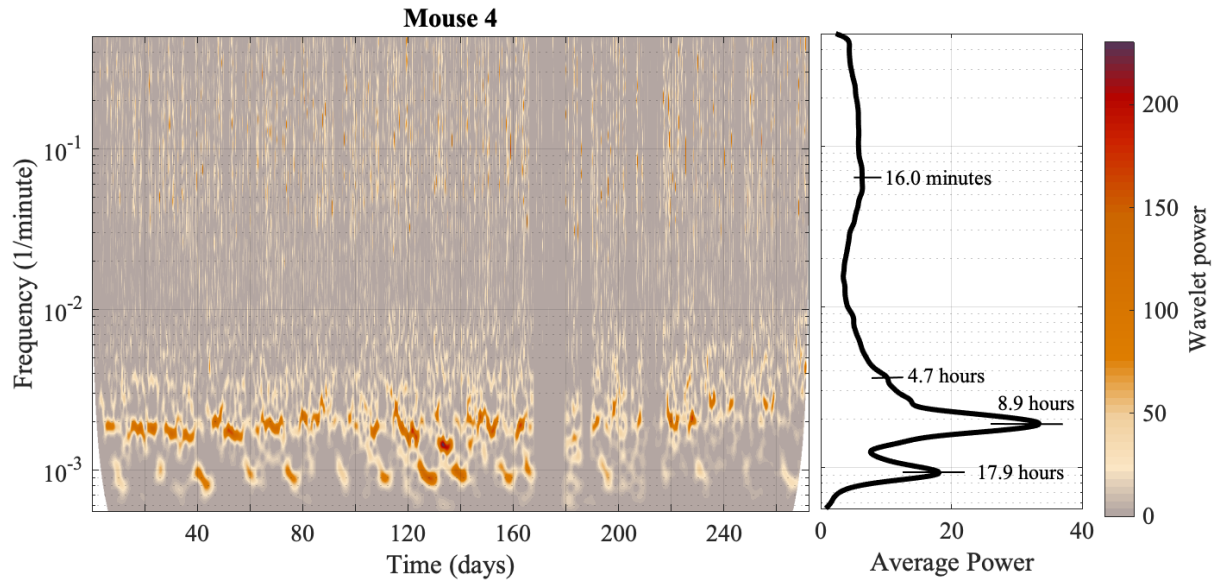


Figure S3: Time-frequency representation of the behavioural data for mice 4 and 5.

1.2 Ridges

The method for extracting ridges from a time-frequency representation introduced by Iatsenko *et al* [2] is used, and the extracted ridges are shown in Figs. S4–S6. The wavelet transform is performed on the behavioural data of all 5 mice. For ridge extraction, the chosen boundaries must contain the entirety of, and only, the oscillatory component under investigation. Both the time-frequency representation and the average power spectrum are used to determine the correct boundaries. The units for wavelet power and the average power are (wheel revolutions/min)².

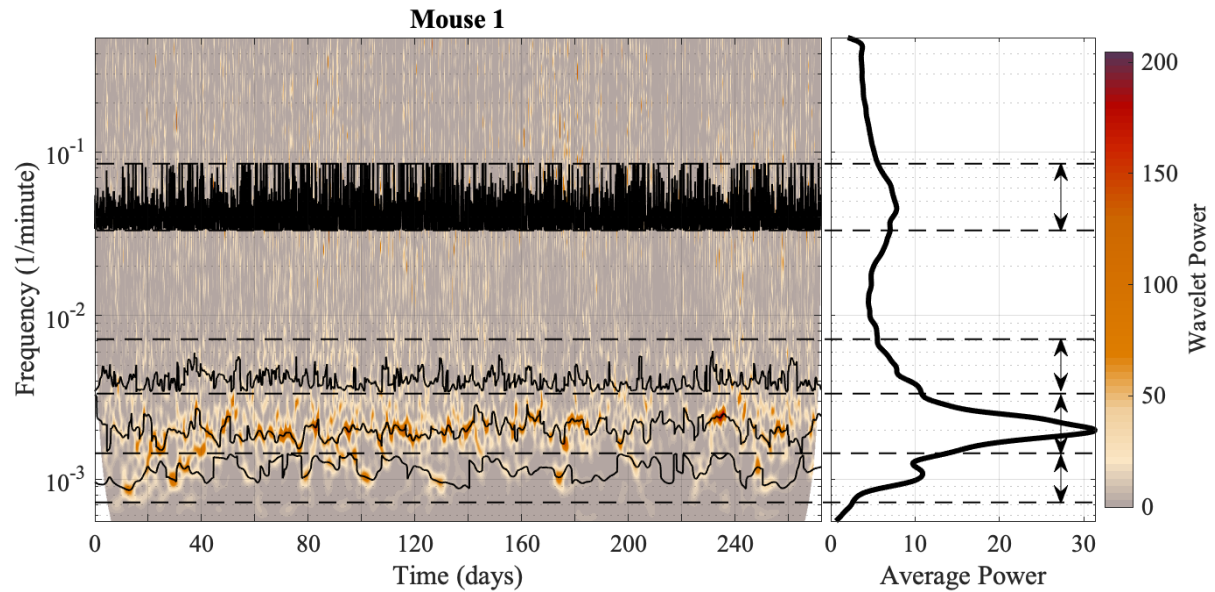


Figure S4: Time-frequency representation of the behavioural data along with the boundaries for ridge extraction, and the extracted ridges for mouse 1.

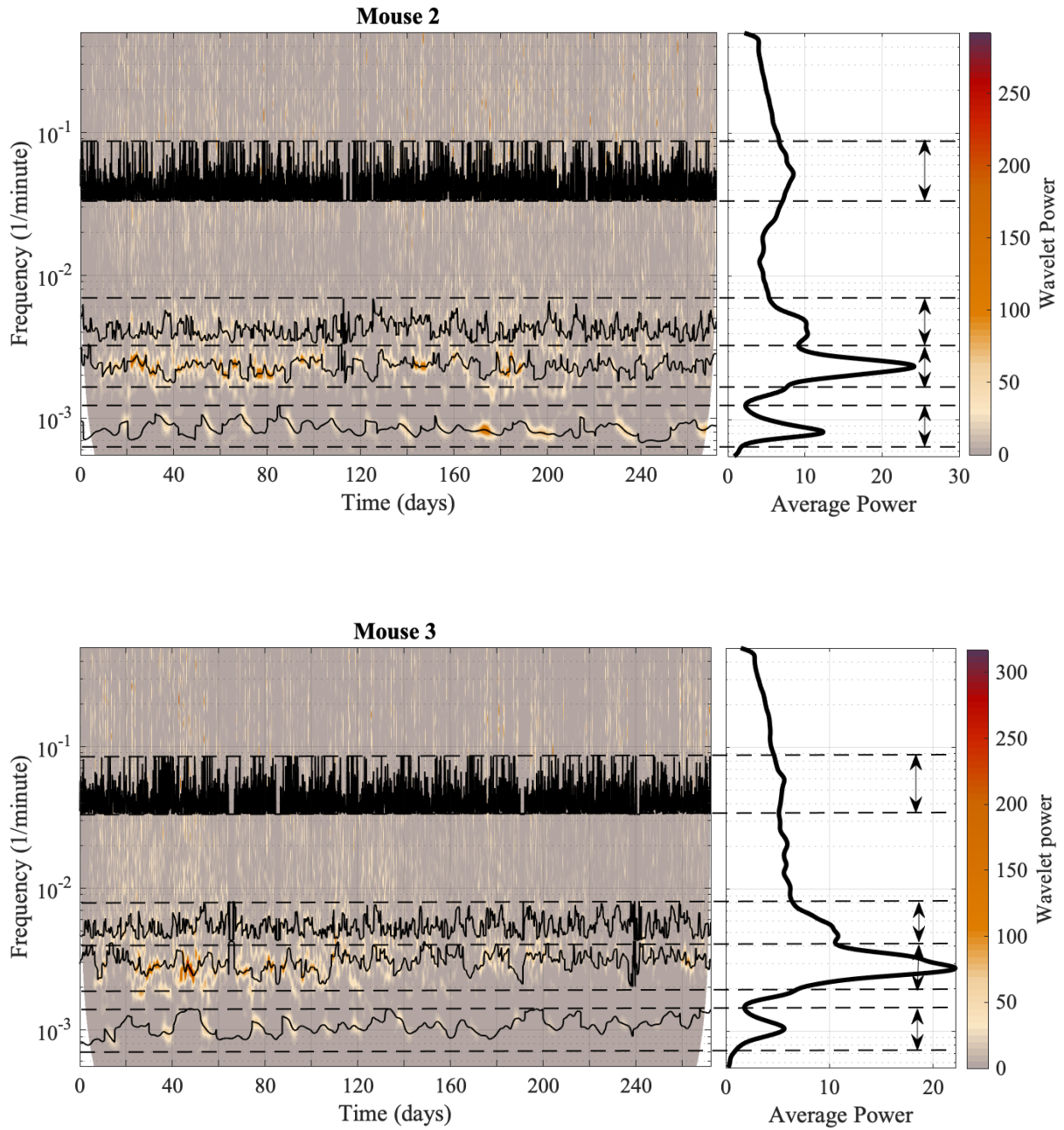


Figure S5: Time-frequency representation of the behavioural data along with the boundaries for ridge extraction, and the extracted ridges for mice 2 and 3.

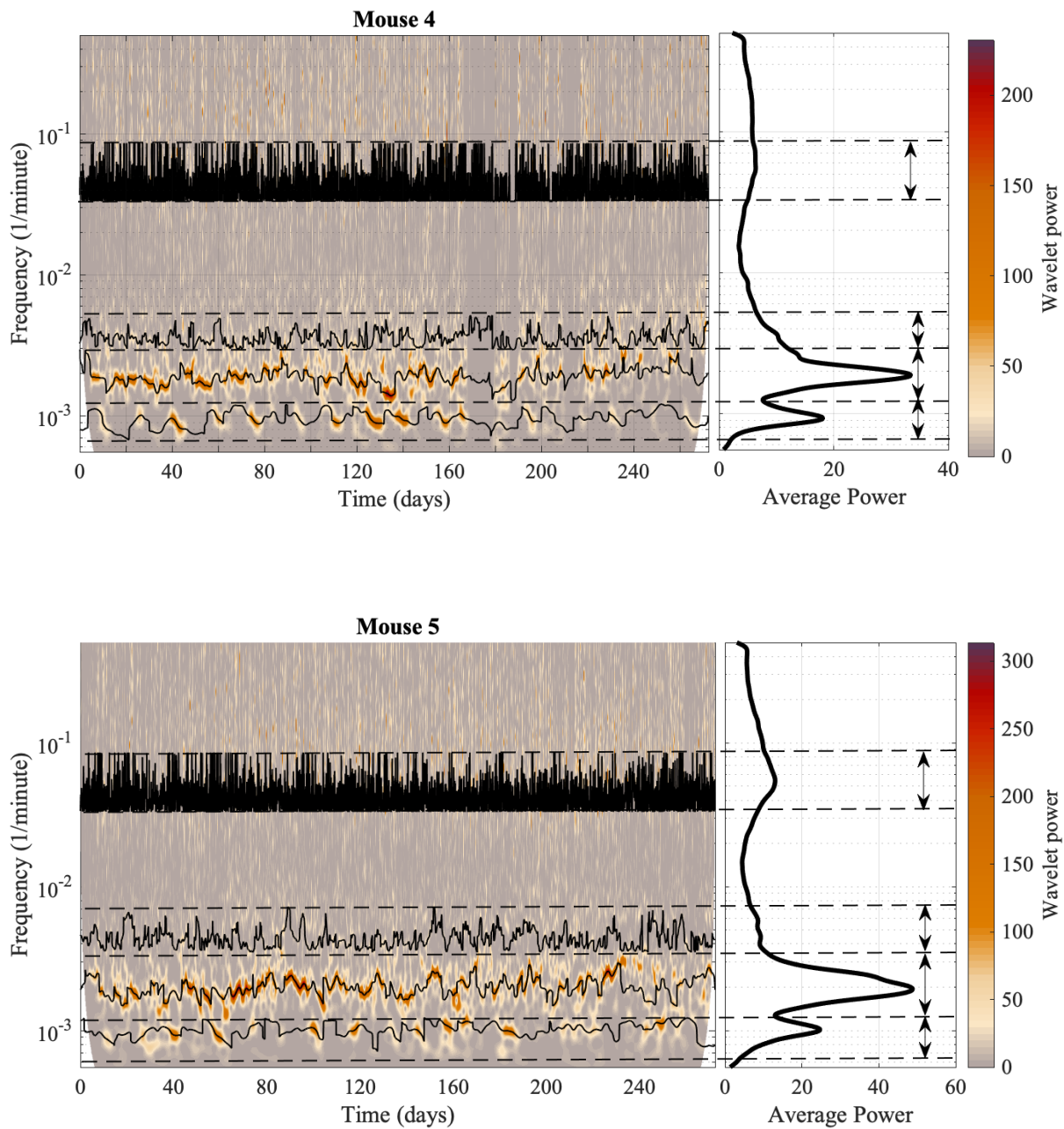


Figure S6: Time-frequency representation of the behavioural data along with the boundaries for ridge extraction, and the extracted ridges for mice 4 and 5.

1.3 Harmonics

The phase time-series of each frequency component are extracted using the wavelet transform, and are compared pairwise. The algorithm, introduced by Sheppard *et al* [3], calculates the mutual information between the pair to determine whether a harmonic relationship exists. The parameters for harmonic algorithm are specified such that harmonics are identified in the frequency-interval of interest, which is in our case from 2 minutes to 27.8 hours. Thus, all previously identified oscillatory components are included in the investigation. The wavelet transform with a time-resolution of 360 minutes is performed to extract phase time-series of each frequency component. 19 amplitude-adjusted Fourier transform (AAFT) surrogates are used. For further detail about methods for hypothesis testing of dynamical systems using surrogate data see [4].

Figures S7–S9 show detected harmonics within the behavioural data of all 5 mice. The plot is a frequency-frequency representation showing which oscillations are in harmonic relationships. The image is symmetric over the diagonal, therefore only half of the figure need to be considered. The frequency boundaries used during ridge extraction for each oscillation detected in the time-frequency representation (oscillation 1, 2, 3 and 4) form the outlines of the dashed boxes in the figure. All of the different combinations of frequencies are investigated, and the boxes are plotted over the harmonic results. The colour-code shows a dimensionless quantity obtained from the actual value, minus the mean of the surrogate distribution, divided by the standard deviation of the surrogate distribution. Negative values correspond to results with values lower than the surrogate mean, therefore significant results are those above 0. For oscillation combinations which overlap with higher-valued areas, the two frequencies are more likely in a harmonic relationship.

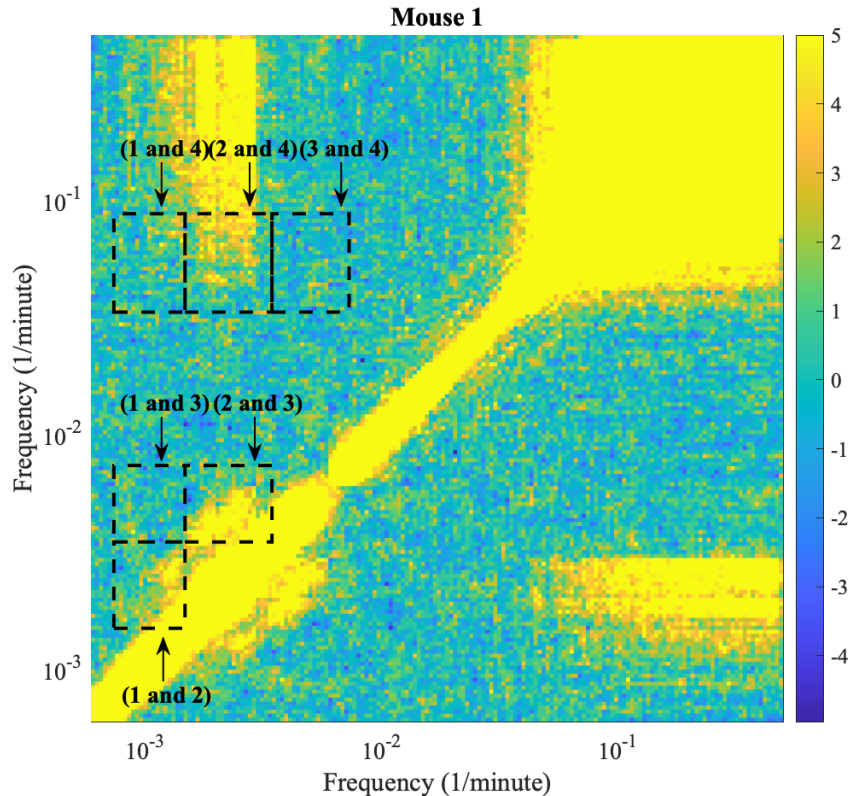


Figure S7: Harmonics analysis of the behavioural data for mouse 1.

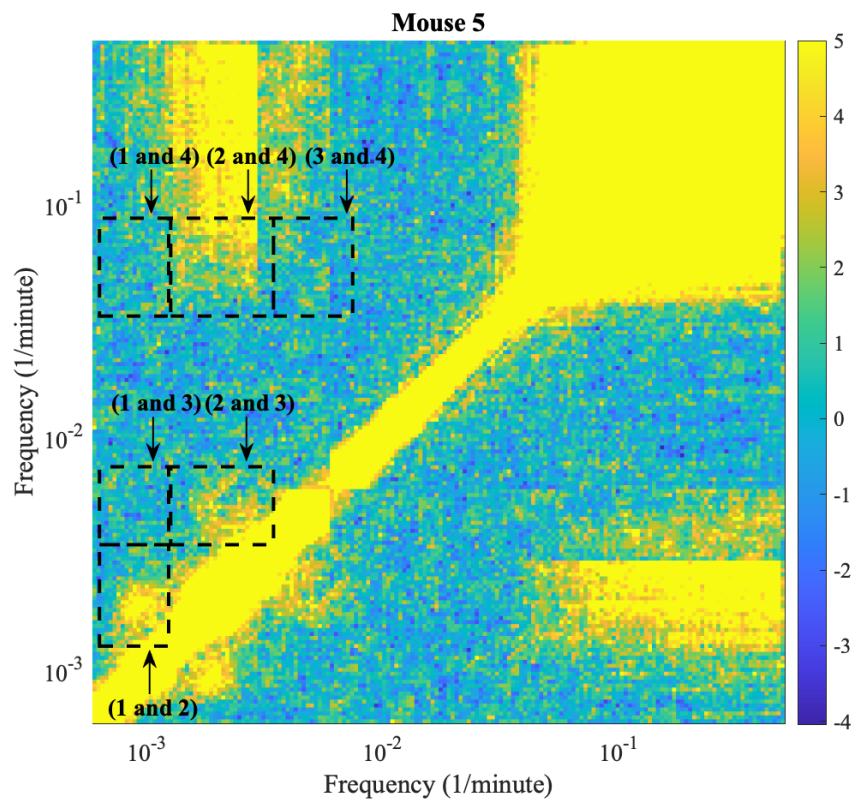
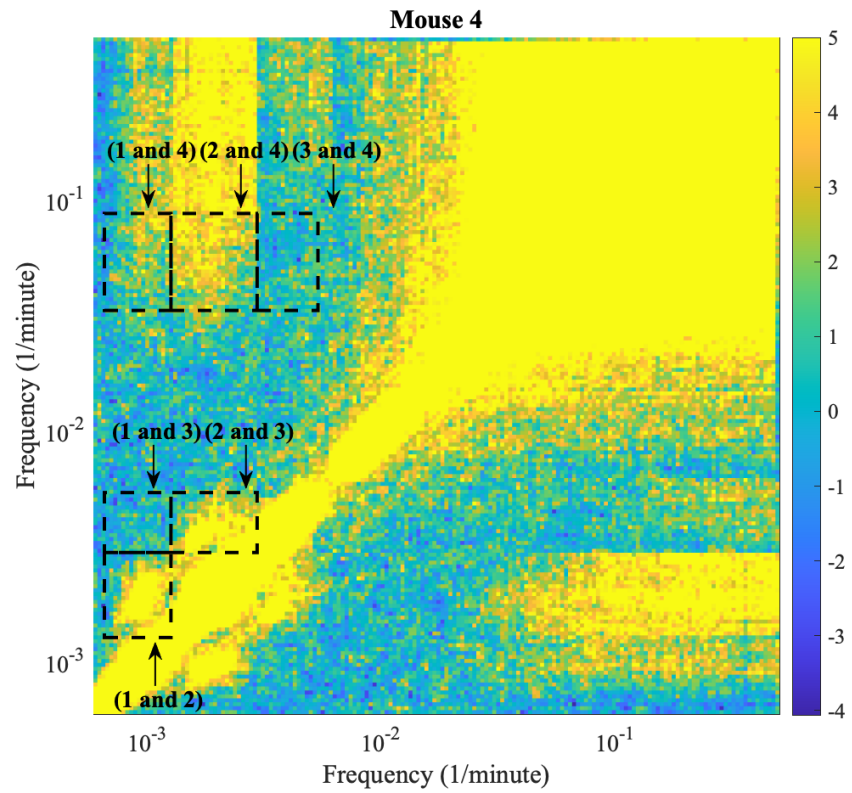


Figure S9: Harmonics analysis of the behavioural data for mice 4 and 5.

1.4 Coupling

The interactions between all combinations of phases of pairs of oscillators for the same animal are investigated. The instantaneous frequencies of an individual oscillatory component are obtained from the time-frequency representation using ridge extraction. The width of the time-windows to determine the time-independent coupling strength are 15880 minutes, and time-windows overlap by 75%. A Fourier order of 2 and a propagation constant of 0.2 is used. 19 cyclic phase permutation (CPP) surrogates are used, and the significance test is performed with a significance level of $\alpha = 0.05$. Figures S10–S14 show the coupling strengths over time between four oscillations (oscillation 1, 2, 3 and 4), within the behavioural data of mouse 1, 2, 3, 4 and 5. The solid lines denote the coupling strength over time, obtained from dynamical Bayesian inference [5]. The dotted lines are the surrogate significance tests. Only results above the surrogate lines are significant. The arrow in the legend denotes the direction of coupling.

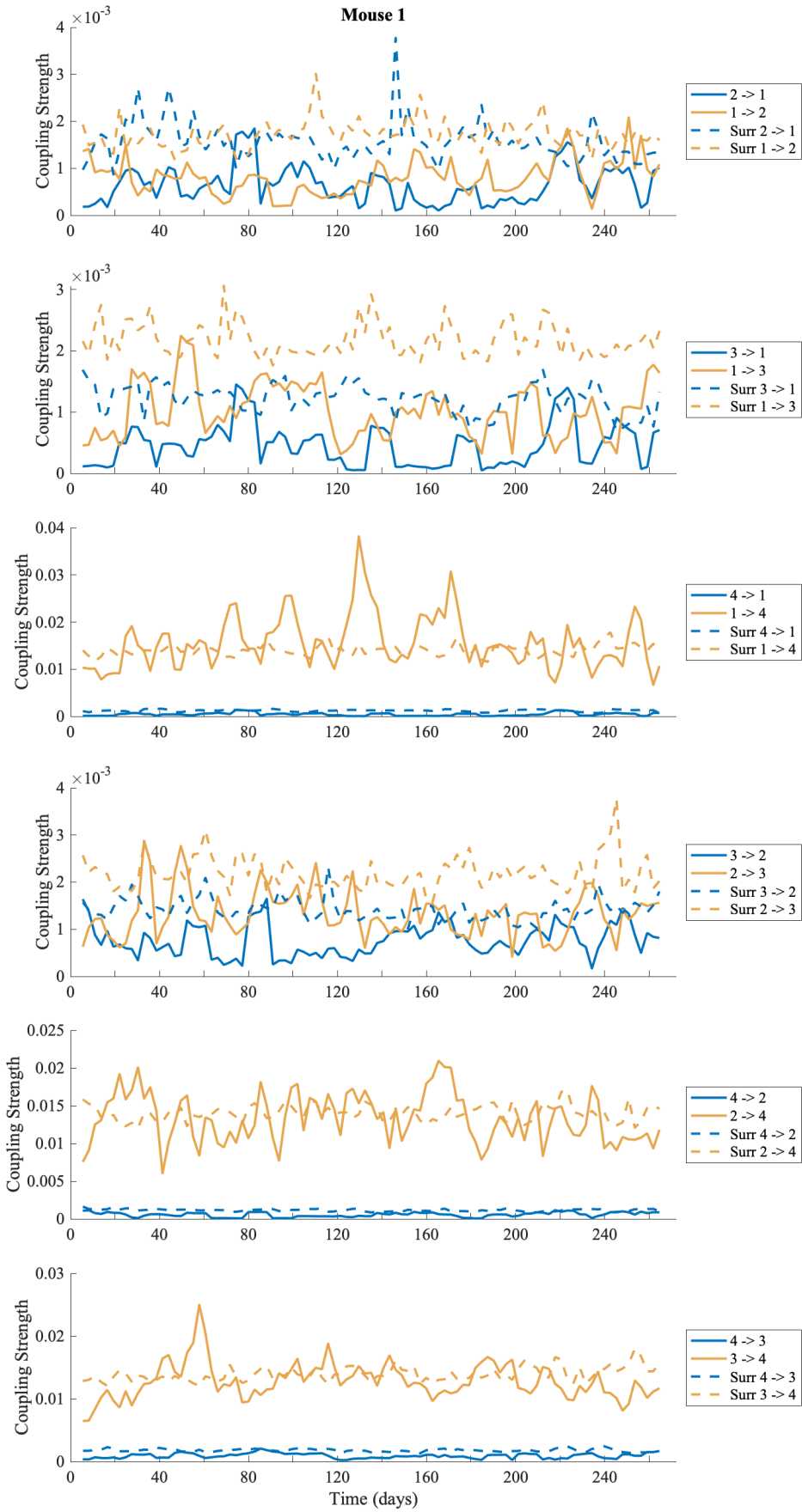


Figure S10: Time-evolution of the coupling strength calculated for mouse 1.

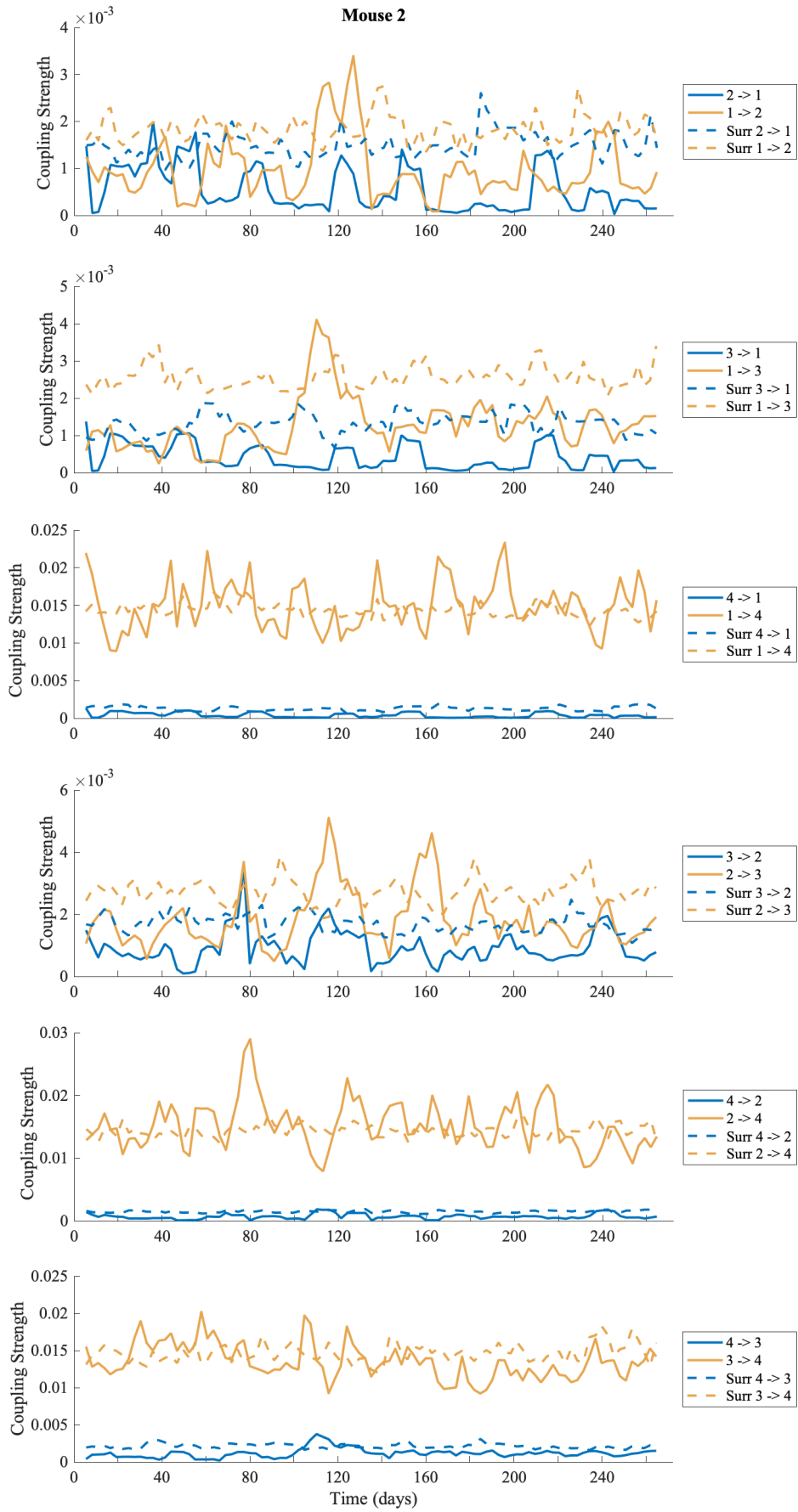


Figure S11: Coupling strength over time calculated for mouse 2.

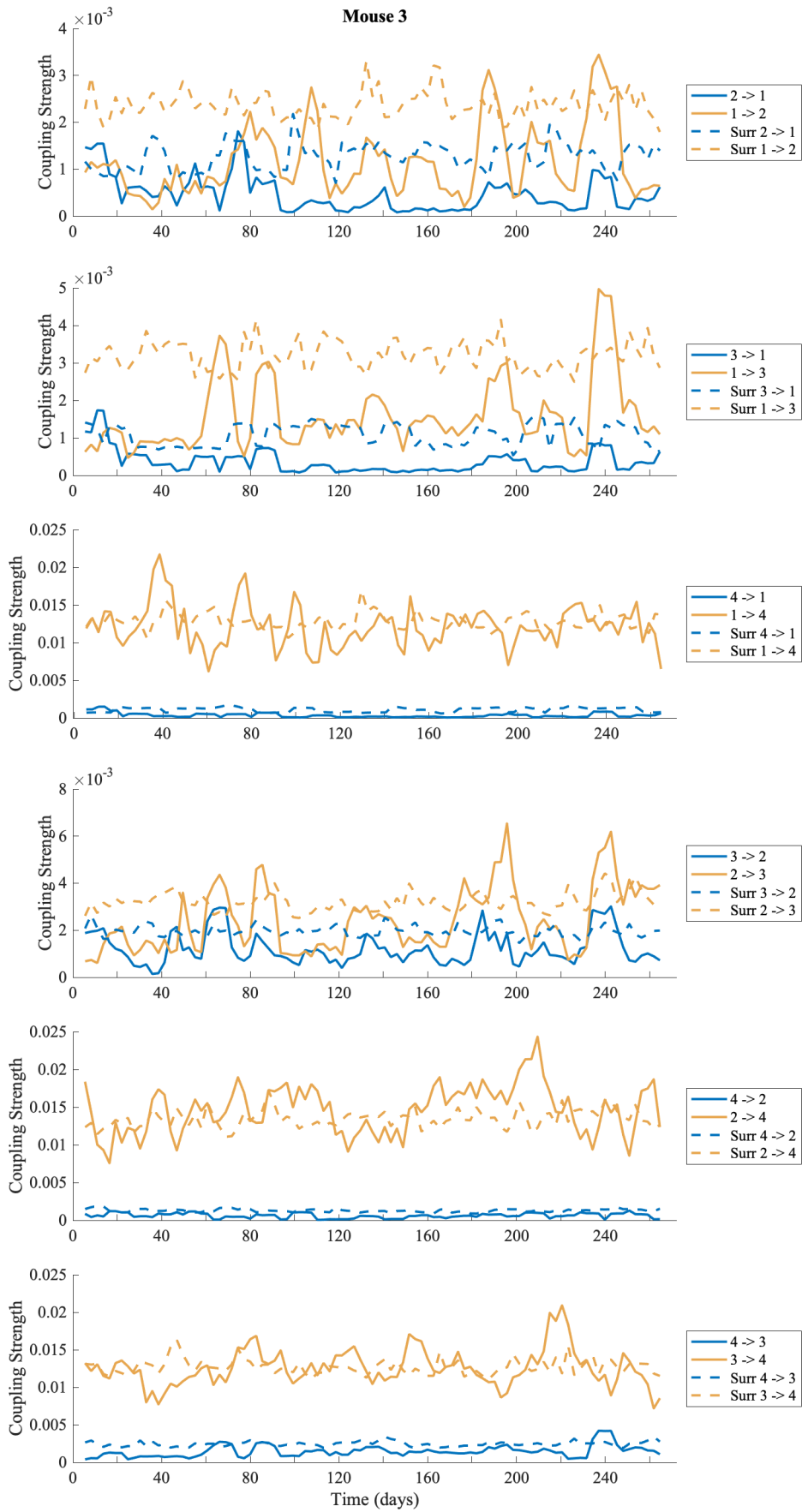


Figure S12: Coupling strength over time calculated for mouse 3.

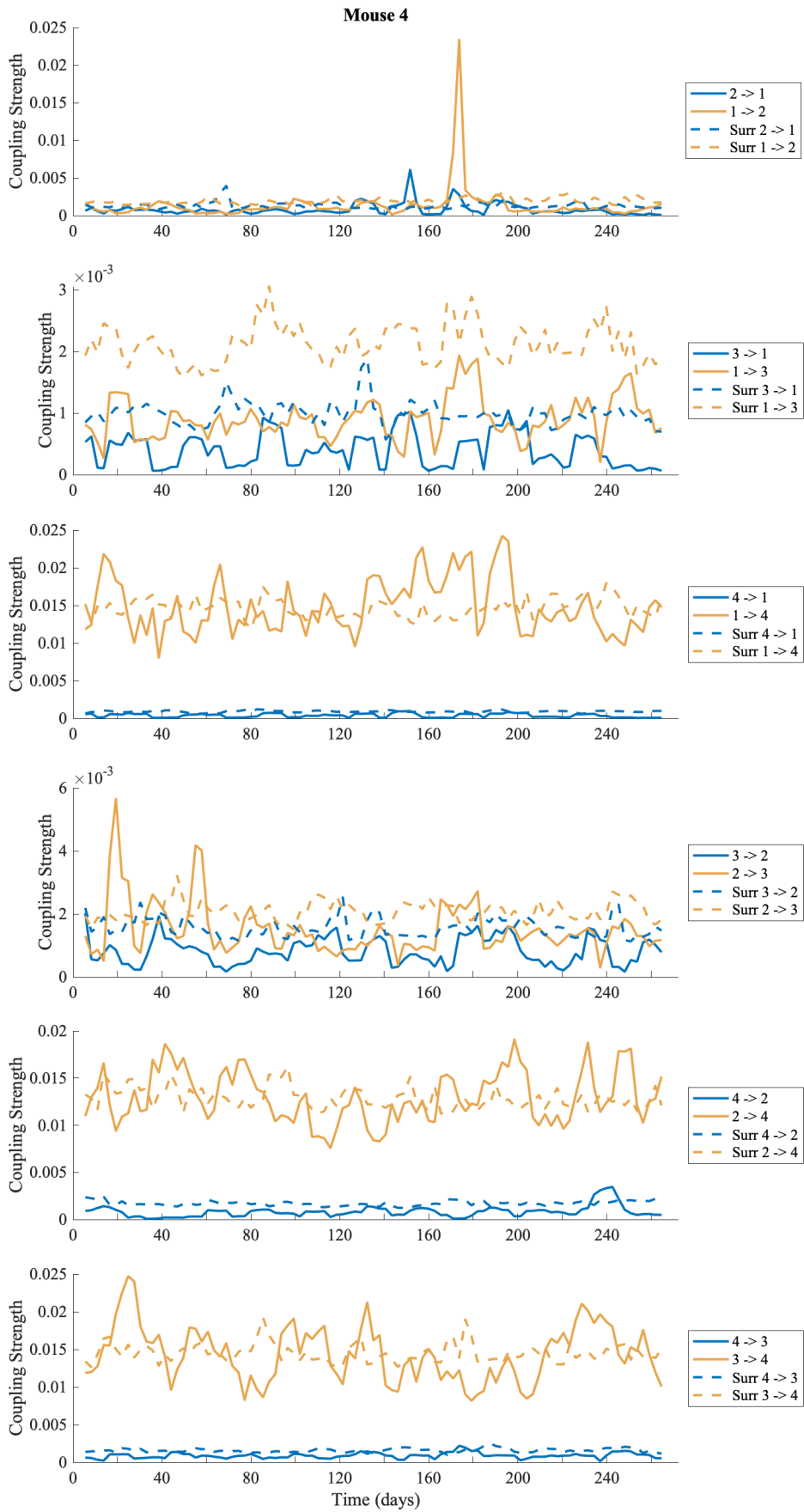


Figure S13: Coupling strength over time calculated for mouse 4.

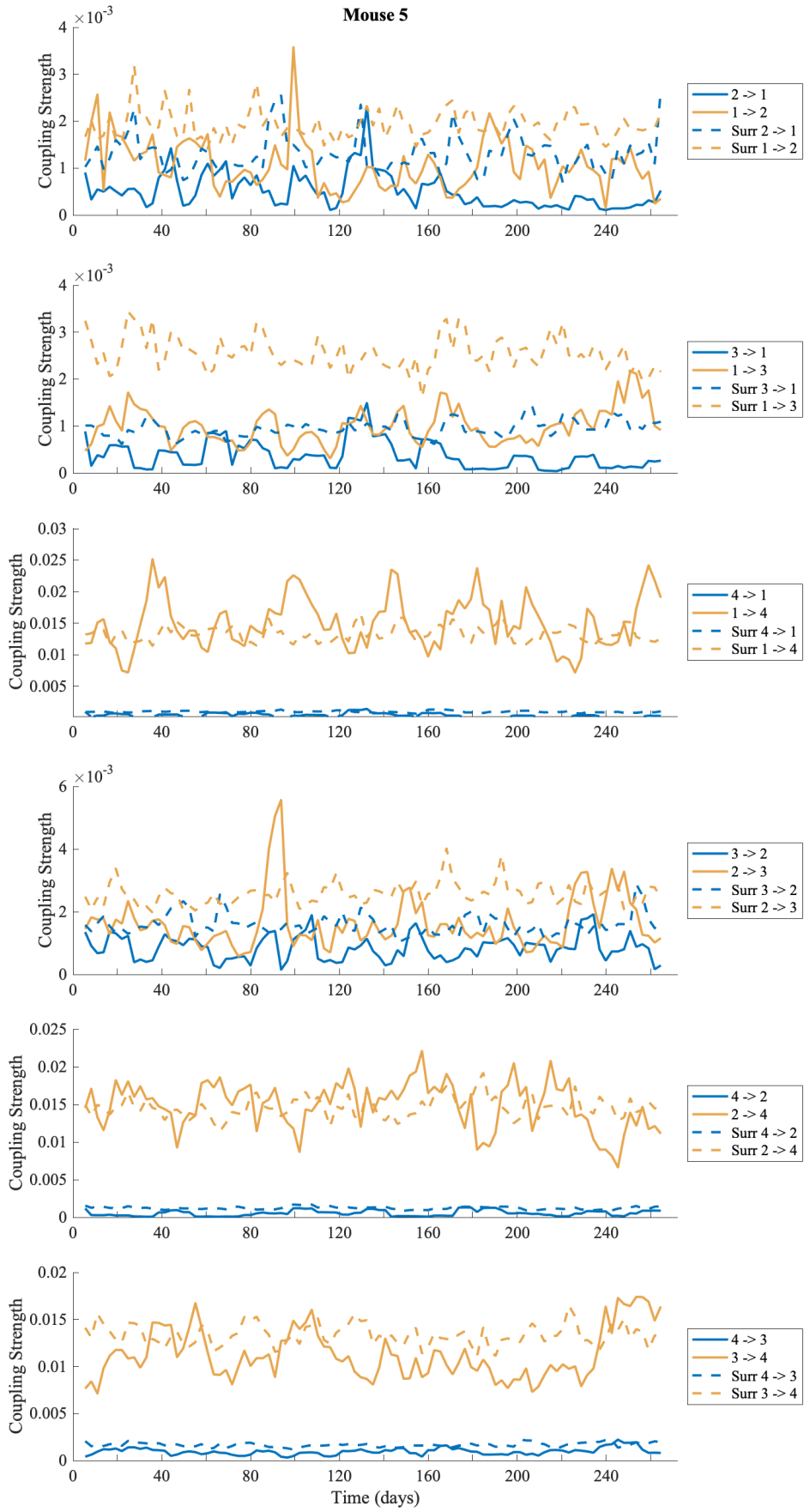


Figure S14: Coupling strength over time calculated for mouse 5.

1.5 Relationship with temperature and humidity

The temperature ($^{\circ}C$) and relative humidity (%) over the time of the experiment, which began in mid-June 2018 and ended in mid-March 2019 in Dallas (Texas) are presented below. Humidity is relatively stable all year around in Dallas, however the large fluctuation in humidity in the last half of recording corresponds to switching air conditioner to heater.

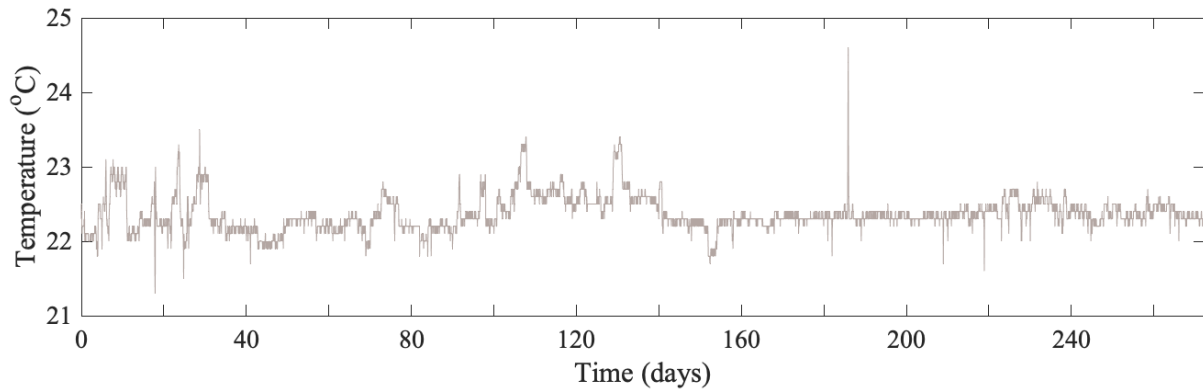


Figure S15: Time -evolution of the ambient temperature during the study

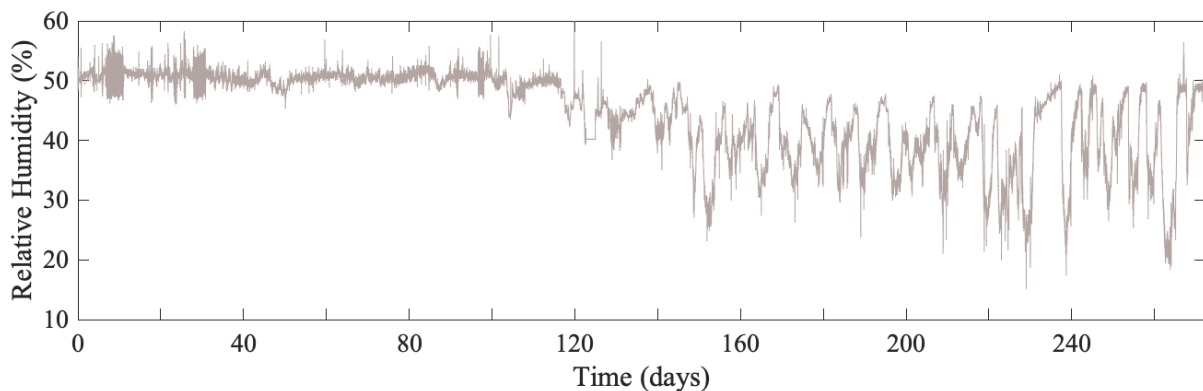


Figure S16: Time-evolution of the relative humidity during the study.

For time-frequency representations of the temperature and relative humidity data, the signals are first detrended. Then, the wavelet transform is applied using the lognormal wavelet and a frequency resolution of 1, for all possible frequencies (2 minutes to ~ 45 days). A cone of influence illustrates logarithmic resolution, i.e. the window within which the wavelet is stretched or contracted changes logarithmically. Hence, for lower frequencies longer windows are used and exponentially longer parts are not included at the beginning and the end of the spectrum. Figures S17 and S18 show the time-frequency representations of temperature and relative humidity, and the corresponding time-averaged power spectrum. The y -axis are presented on a logarithmic scale.

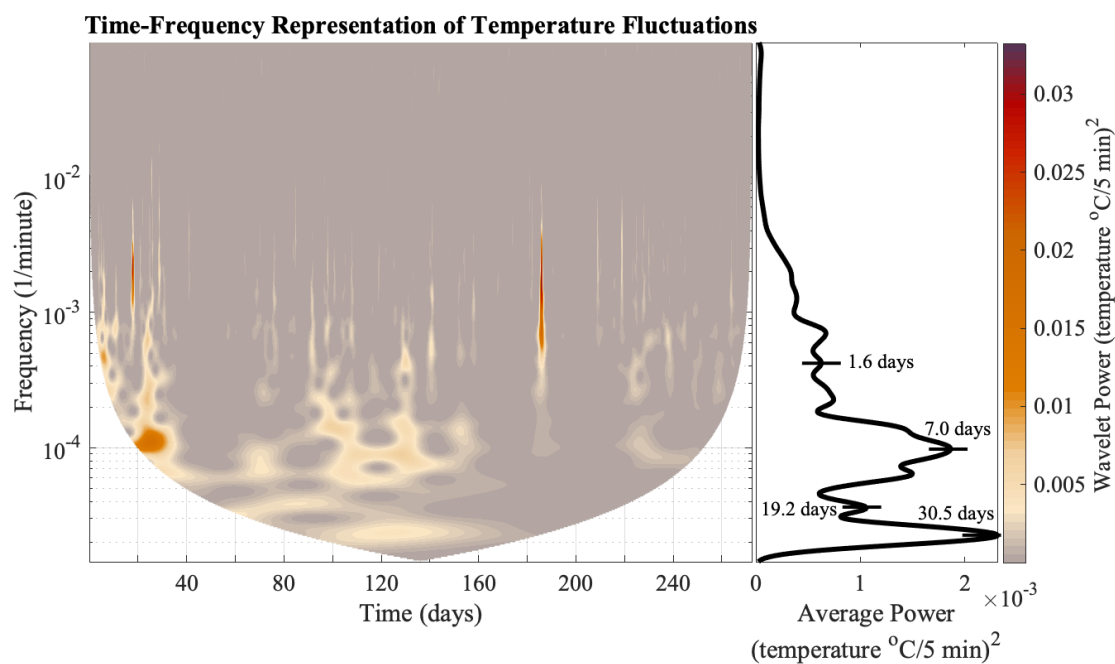


Figure S17: Time-frequency representation (left) and time-averaged wavelet power (right) for room temperature data recorded every 5 min during the study. Note that the extent of fluctuation is very small, as the temperature fluctuation is minimal (22.4 ± 0.4 °C).

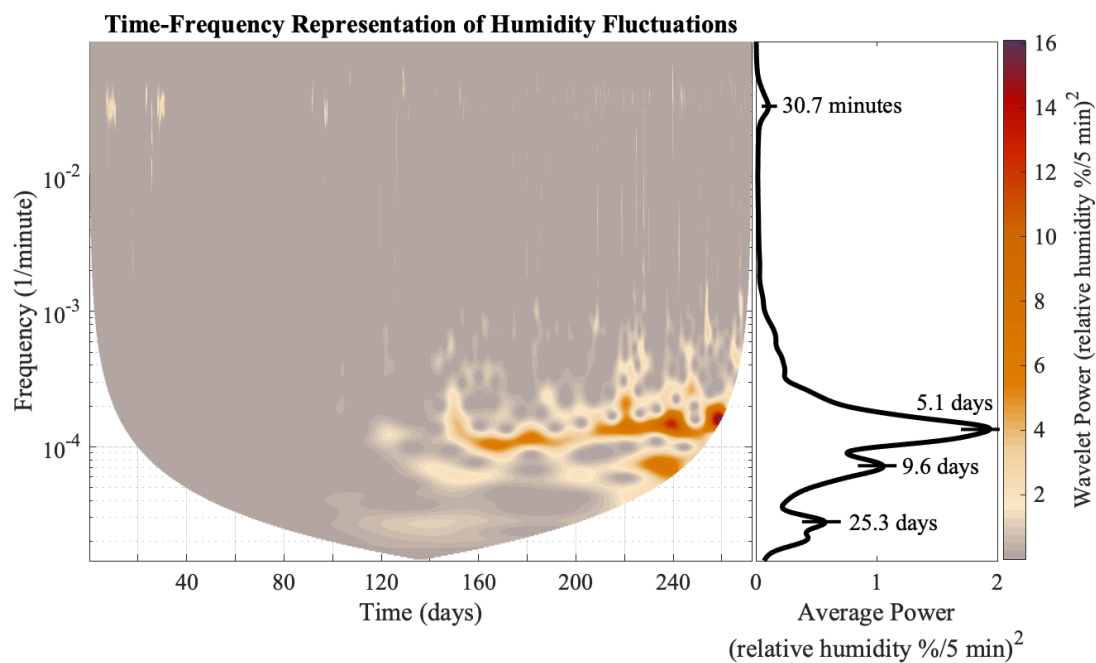


Figure S18: Time-frequency representation of the humidity data (left) and time-averaged wavelet power (right).

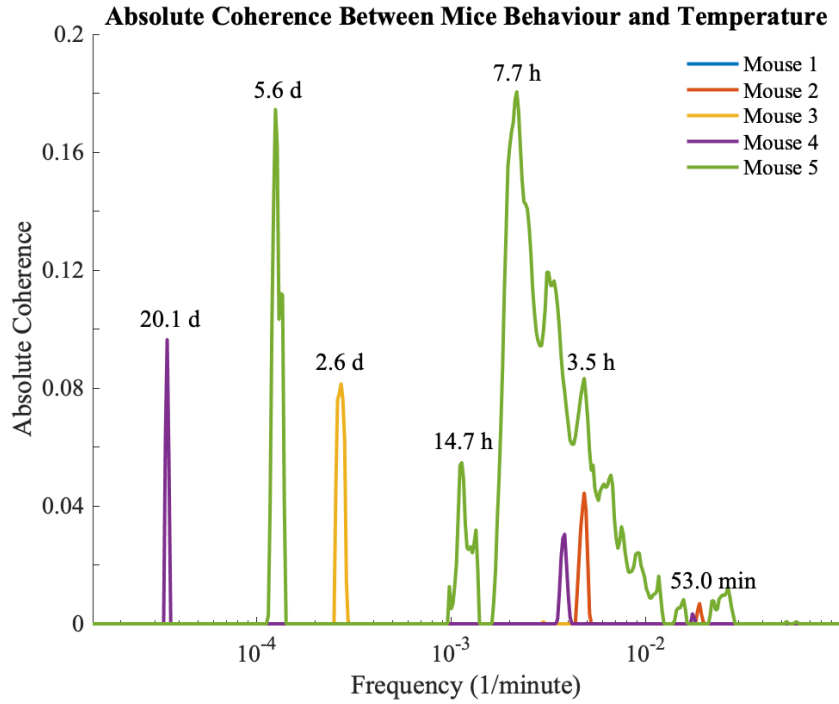


Figure S19: Phase coherence between room temperature fluctuations and mice behavioural data. Mouse 5 is nearest to the sensor.

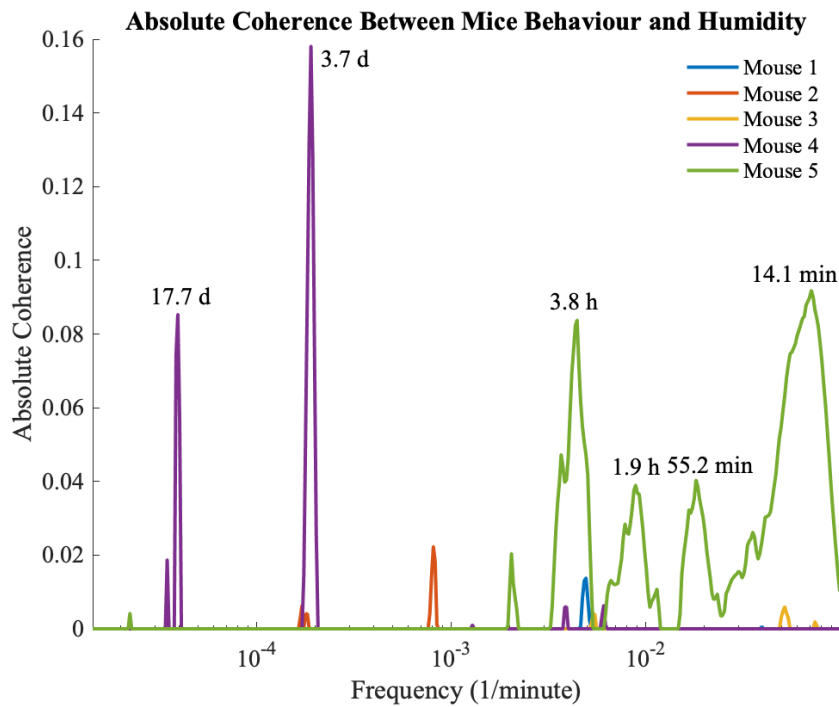


Figure S20: Phase coherence between room humidity fluctuations and mice behavioural data. Mouse 5 is nearest to the sensor.

Wavelet phase coherence was performed between the temperature and humidity data and

each mouse signal, using a lognormal wavelet and a frequency resolution parameter of 1, and over all possible frequencies (2 minutes to ~ 45 days). 60 AAFT surrogates are used. For each mouse for both temperature and humidity, the absolute coherence was calculated by subtracting the surrogate data. All of the significant results are plotted on the same figure, where significant peaks correspond to coherence between the mice and the temperature (Fig. S19) and humidity (Fig. S20). Mouse 5 has significant coherence with temperature and humidity at a range of frequencies, and this may be due to the smaller distance between mouse 5 and the temperature/humidity sensor, which may pick up the temperature and humidity of mouse 5.

References

- [1] D Iatsenko, P V E McClintock, A Stefanovska (2015) Linear and synchrosqueezed time-frequency representations revisited: Overview, standards of use, resolution, reconstruction, concentration, and algorithms, *Digital Signal Processing* **42**, 1–26.
- [2] D Iatsenko, P V E McClintock, A Stefanovska (2016) Extraction of instantaneous frequencies from ridges in time-frequency representations of signals, *Signal Processing* **125**, 290–303.
- [3] L W Sheppard, A Stefanovska, P V E McClintock (2012) Testing for time-localized coherence in bivariate data, *Phys Rev E* **85**, 046205.
- [4] G Lancaster, D Iatsenko, V Ticcinelli, A Pide, A Stefanovska (2018) Surrogate data for hypothesis testing of dynamical systems, *Phys Rep* **748**, 1–60.
- [5] T Stankovski, A Duggento, P V E McClintock, A Stefanovska (2014) A tutorial on time-evolving dynamical Bayesian inference, *European Physical Journal – Special Topics* **223**, 2685–2703.